PHOTOSYNTHETICA
International Journal for Photosynthesis Research

DOI 10.32615/ps.2021.008 PHOTOSYNTHETICA 59 (1): 137-147, 2021

Adaptation of *Amorpha fruticosa* to different habitats is enabled by photosynthetic apparatus plasticity

S. MLINARIĆ[*], T. ŽUNA PFEIFFER[*,+], Lj. KRSTIN[*], D. ŠPOLJARIĆ MARONIĆ[*], M. OŽURA[**], F. STEVIĆ[*], and M. VARGA[*]

Department of Biology, Josip Juraj Strossmayer University of Osijek, Cara Hadrijana 8/A, HR-31000 Osijek, Croatia[*]
Karlovac University of Applied Sciences, Trg Josipa Jurja Strossmayera 9, HR-47000 Karlovac, Croatia[**]

Abstract

The rapid growth and spreading of invasive plant species could be related to their efficient photosynthesis performance. We analysed and compared photosynthetic efficiency of invasive indigo bush (*Amorpha fruticosa* L.) and noninvasive native *Quercus robur* L., *Alnus glutinosa* L., *Populus alba* L., and *Cornus sanguinea* L. with the overlapping distribution. The study was performed at two lowland areas at the beginning of the vegetation season (May) and during the flowering period (July). At both study sites, indigo bush showed better photosynthetic performance than native plants. Negative L- and K-bands in indigo bush indicated faster electron transport and better connectivity within the PSII units. Additionally, the highest performance and structure–function indexes suggested efficient utilization of absorbed light energy in indigo bush. Our results suggested that remarkable plasticity of photosynthetic reactions in indigo bush enabled them more efficient capture and utilization of light energy what might be important factors contributing to the invasiveness of this alien species.

Keywords: indigo bush; K-band; L-band; photosynthetic plasticity; structure–function index.

Highlights

- Invasive indigo bush showed exceptional plasticity of photosynthetic apparatus
- Indigo bush revealed more enhanced electron transport than accompanying native species
- Successful adaptation arises from efficient capture and utilization of light resources

Received 28 July 2020
Accepted 25 January 2021
Published online 18 February 2021

[+]Corresponding author
e-mail: tzuna@biologija.unios.hr

Abbreviations: ABS – absorption flux; ABS/RC – absorption flux per active RC; ChlF – chlorophyll *a* fluorescence; DF_{ABS} – total driving force; DI_0/RC – dissipation flux per active RC; ET_0/RC – electron transport flux per active RC; F_0 – minimal fluorescence intensity; F_{300} – fluorescence intensity at 300 μs; F_I – fluorescence intensity at 2 ms; F_J – fluorescence intensity at 30 ms; F_m – maximal fluorescence intensity; F_v – maximal variable fluorescence; F_v/F_m – maximum quantum yield for primary photochemistry; LSD – *Fisher*'s least significant difference test; M_0 – approximated initial slope of relative variable fluorescence F_v; OEC – oxygen-evolving complex; PB – Pokupsko basin; PI_{ABS} – performance index on absorption basis; PQ – plastoquinone; RC – reactive centre; RE_0/RC – electron flux reducing end electron acceptors at the PSI acceptor side, per RC; TR_0/RC – trapping flux per active RC; V_I – relative variable fluorescence at 30 ms (I-step); V_J – relative variable fluorescence at 2 ms (J-step); V_K – relative variable fluorescence at 300 μs (K-step); V_L – relative variable fluorescence at 150 μs (L-step); V_t – relative variable fluorescence at time t; ZU – Županja area; ΔDF_{ABS} – relative changes in the difference of driving forces; ΔW_{OP} – difference kinetics between O- and P-steps; ΔW_{OJ} – difference kinetics between O- and J-steps; ΔW_{OK} – difference kinetics between O- and K-steps; δ_{R0} – efficiency/probability with which an electron from the intersystem electron carriers moves to reduce end electron acceptors at the PSI acceptor side; φ_{E0} – quantum yield of electron transport from Q_A^- to PQ; φ_{P0} – maximum quantum yield of PSII; φ_{R0} – quantum yield of electron transport from Q_A^- to final PSI acceptors; ψ_{E0} – efficiency that trapped electron is transferred from Q_A^- to PQ.

Acknowledgments: The authors are grateful to Tamara Jakovljević (Croatian Forest Research Institute, Croatia) for soil analysis and to prof. Vera Cesar for the laboratory equipment. We also wish to thank to Matej Šag and Nikolina Bek for field and laboratory assistance.
Conflict of interest: The authors declare that they have no conflict of interest.

Introduction

In the recent decades, a number of invasive non-native plant taxa have been spread worldwide (Genovesi *et al.* 2010), severely influencing ecosystem services (Vilà *et al.* 2010), economy (Keller *et al.* 2011), and biodiversity (Hejda *et al.* 2009, Dogra *et al.* 2010). Although the mechanisms of plant invasiveness are still not thoroughly understood, it is considered that in a new environment, non-native taxa liberated from natural enemies, may grow and reproduce rapidly, becoming superior competitors for essential resources than native plants (Keane and Crawley 2002, Levine *et al.* 2003, Dudeque Zenni *et al.* 2016). They have a high potential for acclimation that enables them to become abundant in a wide range of habitat types (Shi and Ma 2006, Mayer *et al.* 2017, Luo *et al.* 2019).

The higher photosynthetic rate was recognized as one of the most important mechanisms allowing invasive plants to achieve a success in a variety of environmental conditions (Bajwa *et al.* 2016, Le *et al.* 2019). The estimation of plant physiological status under natural conditions is an important aspect of monitoring and detection of plant responses and its survival under stressful conditions. Over the last few decades, the chlorophyll (Chl) *a* fluorescence has been widely used as a noninvasive, very sensitive, and fast method for estimation of photosynthetic performance under such conditions that can provide a reliable source of information on plant condition (Goltsev *et al.* 2016, Bussotti and Pollastrini 2017, Mlinarić *et al.* 2017, Pollastrini *et al.* 2017, Kalaji *et al.* 2018, Žuna Pfeiffer *et al.* 2018).

The photosynthetic performance can be determined using the JIP-test, based on the fast rise of Chl fluorescence after exposure of the sample to photosynthetic active light (Strasser *et al.* 2000, Govindjee 2004, Papageorgiou 2004, Schansker *et al.* 2014, Kalaji *et al.* 2018). In the dark conditions, all photosynthetic reaction centres (RCs) as well as the electron transport chain between PSII and PSI are open (O), meaning that plastoquinone A (Q_A), plastoquinone B (Q_B), and the pool of free plastoquinones (PQ) behind the PSII RCs are completely oxidised, and the fluorescence intensity of the system is minimal (F_0). After illumination of the sample, electrons migrate *via* Q_A and Q_B to the PQ pool, increasing the fluorescence emission intensity represented as sigmoidal shaped OJIP curve that reflects the redox state of Q_A and Q_B. The reduction of all Q_A molecules represents the J-step, while the reduction of all Q_B represents the I-step. Two additional time-bands, L- and K-band reflect the energetic connectivity between PSII units and the state of oxygen-evolving complex (OEC), respectively (Yusuf *et al.* 2010). The peak of fluorescence intensity (P) is reached when the PQ pool is completely reduced (Strasser *et al.* 2004, Küpper *et al.* 2019). Previously, the most used parameter was F_v/F_m that served for the estimation of the maximum quantum yield of primary photochemistry (Zhou *et al.* 2015, Begović *et al.* 2016, Mlinarić *et al.* 2016, 2017; Zhao *et al.* 2017). However, several other parameters derived from F_0 and F_m but also from fluorescence levels at J-, I-, K-, and L-steps, provide information on the structure and function of PSII (Stirbet *et al.* 2018). Performance index (PI_{ABS}) is one of the most widely used parameters that describes the effectiveness of electron transport to the PQ pool. Driving forces (DF) estimate the global driving strength of processes evaluated by the corresponding PI_{ABS}, while the structure–function index (SFI_{ABS}) characterizes structural and functional characteristics of PSII (Strasser *et al.* 2004, Stirbet *et al.* 2018).

Indigo bush (*Amorpha fruticosa* L.), deciduous shrub from the Fabaceae family, is one of the widely distributed invasive species (Sărăţeanu 2010, Gudžinskas and Žalneravičius 2015, Petrović *et al.* 2016, Vincetić *et al.* 2017). The plant is native to the North America where it occupies a variety of habitats including wet woods, moist ground near streams and ponds, rocky banks, and ravines (DeHaan *et al.* 2006). Indigo bush has a high tolerance to various habitat conditions promoting its aggressive invasive behaviour outside of its native range. It is successful in colonising abandoned agricultural and disturbed wetland habitats as well as creating effective vegetative cover at ash lagoons of thermoelectric plants due to its ecophysiological characteristics and high photosynthetic efficiency (Mitrović *et al.* 2012). At invaded sites, indigo bush affects microclimate, vegetation structure, composition, and abundance of soil invertebrates (Brigić *et al.* 2014). Due to the allelopathic potential, it reduces the germination and seedling growth (Csiszár *et al.* 2013) and represents an important limiting factor for forest regeneration (Jakovljević *et al.* 2015, Horvat and Franjić 2016).

The study aimed to analyse and compare the photosynthetic performance of indigo bush and native woody species growing in the same habitat conditions. It has been found that some invasive plants may have a higher maximum photosynthetic rate (McDowell 2002, Feng *et al.* 2007), increased thermostability of their photosynthetic apparatus, and more efficient regulating mechanism in energy partitioning of PSII than the noninvasive species belonging to the same genus (Song *et al.* 2010). Based on that, we assumed that indigo bush, an invasive species, performs better and that it could adapt its photosynthetic response according to the specific site conditions. Our investigation results could contribute to a better understanding of mechanisms that play a role in the success of this invasive species and additionally, for the development of appropriate control strategies.

Materials and methods

Study sites and plant species: The study was conducted at the two locations: in a lowland oak forest, a part of the Pokupsko basin (PB) forest complex (45°36'N, 15°41'E; the central part of Croatia, located approximately 35 km SW of Zagreb) and in the lowland area of East Croatia in the vicinity of the town Županja (ZU; 45°07'N, 18°70'E). At every location, three study sites were chosen due to the high occurrence of indigo bush (Table 1).

In both locations, the climate has a characteristic moderate continental climate with hot summers and cold winters. Meteorological data for both study sites were

Table 1. Study sites characteristics.

Study site		Pokupsko basin			Županja area		
		PB1	PB2	PB3	ZU1	ZU2	ZU3
Coordinates	N	45°54'11.18"	45°52'28.56"	45°53'22.48"	45°05'33.02"	45°03'36.04"	45°05'25.67"
	E	15°73'31.08"	15°71'76.24"	15°62'30.81"	18°41'13.24"	18°42'51.45"	18°42'33.63"
Habitat type		forest edge	meadow edge	the shore of the pond	embankment	along the agricultural areas	
Investigated species		*Amorpha fruticosa* *Quercus robur* *Alnus glutinosa*			*Populus alba*		*Cornus sanguinea*
Precipitation [mm]	Annual	97.35			64.75		
	May	110.61			86.59		
	July	87.46			64.24		
Temperature [°C]	Annual	11.24			12.36		
	May	16.28			17.74		
	July	22.03			23.43		
Soil composition							
pH	H_2O	7.51	6.18	7.67	7.54	7.72	6.45
	1 M KCl	6.94	4.53	7.19	7.00	7.32	5.12
P_2O_5 [mg 100 g^{-1}(soil)]		6.71	0.94	1.23	23.53	26.40	1.63
K_2O [mg 100 g^{-1}(soil)]		10.59	8.90	10.95	34.32	33.44	14.26
N [%]		0.41	0.41	0.14	0.38	0.14	0.34
Humus [%]		5.24	5.31	2.53	5.45	1.61	4.62
C [%]		3.05	3.09	1.47	3.17	0.94	2.69
C/N [%]		7.44	7.54	10.5	8.34	6.71	7.91
$CaCO_3$ [%]		4.13	0	23.95	9.27	13.91	0
Sand (0.63–2 mm) [%]		5.27	4.67	23.54	6.82	27.93	1.87
Dust (0.002–0.063 mm) [%]		39.2	41.65	34.65	50.58	40.96	39.92
Clay (< 0.002 mm) [%]		55.53	53.68	41.81	42.60	31.11	58.21
Soil texture		clay	powdery clay soil	clay	powdery clay soil	clay loam	clay

provided by the Meteorological and Hydrological Service of Croatia for the 15-year period (2001–2016). The dominant tree species in the Pokupsko basin is common oak (*Quercus robur* L.) with a significant share of other species including common hornbeam (*Carpinus betulus* L.), black alder (*Alnus glutinosa* (L.) Geartn.), narrow-leafed ash (*Fraxinus angustifolia* Vahl.), common hazel (*Corylus avellana* L.), and hawthorn (*Crateagus monogyna* Jacq.). The Županja area consists of a very complex landscape with agricultural fields, forest vegetation, shrubs, abandoned agricultural lands, and melioration channels alternated to roads, settlements, and industrial sites. The forests of common oak with great green weed (*Genisto elatae–Quercetum roboris*) as well as the forests of common oak and common hornbeam (*Carpino betuli–Quercetum roboris*) are widespread in this lowland area (Pokos and Turk 2012).

In both PB and ZU, the three different habitat types (Table 1), characterized by dense stands of indigo bush shrubs were chosen. At least five one-year-old indigo bush shrubs of the same size were chosen per the investigated area. To compare the photosynthetic performance of invasive indigo bush to those of native species, we studied woody plants that commonly co-occur with indigo bush at each site – common oak (*Quercus robur*) and black alder (*Alnus glutinosa*) in Pokupsko basin, as well as white poplar (*Populus alba* L.) and common dogwood (*Crataegus sanguinea* L.) in the area of Županja (Table 1). All co-occurring species were approximately of the same size as indigo bush shrubs.

Field sampling and measurement: Soil sampling at each location was carried out at the beginning of the investigation in May 2017. Three soil subsamples were collected randomly using a quadrat size (5 × 5 m) at a depth of 30 cm in the upper layer of the pedosphere. Basic chemical properties of the composed sample, such as soil pH (ISO 10390), soil organic matter (ISO 14235), and plant-available N, P, and K (Table 1) were analysed (Egnér *et al.* 1960).

The Chl *a* fluorescence (ChlF) transient measurement (JIP-test) was performed *in situ* using a *Handy PEA*

(*Hansatech Instruments Ltd.*, Norfolk, UK). ChlF was measured in fully expanded leaves of each plant species at the beginning of vegetation season in May and during the flowering period in July 2017. At least five plants of each species were used for measurements. Randomly selected leaves (n = 25) from each studied plant species were dark-adapted for at least 30 min before measurements. All measured leaves were selected from the shaded part of the canopy to avoid possible photoinhibition. ChlF transients were induced by applying the pulse of saturating red light [peak at 650 nm; 3,000 μmol(photon) m^{-2} s^{-1}] and the data were recorded from 20 μs to 1 s. Recorded ChlF transients were analysed using the JIP-test (Strasser *et al.* 2000, 2004; Yusuf *et al.* 2010). Calculations and descriptions of used parameters are shown in Appendix.

Statistical analyses: Statistical differences between fluorescence measurements in the invasive indigo bush and native species measured in May and July were analysed using the factorial analysis of variance (*ANOVA*) followed by post-hoc *Fisher*'s least significant difference (LSD) test. Differences were considered significant at p<0.05. For fluorescence measurements, each data point represents the mean ± standard deviation of 25 replicates (n = 25). Calculated fluorescence parameters (except for PI_{ABS}) were normalised to measurements in May to compare differences between species at each investigated area.

Results

The amount of precipitations and the soil composition at the investigated sites indicated differences in habitat conditions (Table 1). The highest precipitation amount was recorded in the Pokupsko basin (PB). According to texture, the soil of the forest habitats in PB was classified as clay and was characterised by relatively low content of nutrients [*e.g.*, 0.94–6.71 mg(P_2O_5) 100 g^{-1}(soil); 8.9–10.95 mg(K_2O) 100 g^{-1}(soil)]. In the area of Županja (ZU) soil texture varied and the soil was classified as powdery clay soil, clay loam, and clay. At the ZU1 and ZU2 sites the content of P_2O_5 (ZU1: 23.53 mg 100 g^{-1}; ZU2: 26.40 mg 100 g^{-1}), as well as the content of K_2O (ZU1: 34.32 mg 100 g^{-1}; ZU2: 33.44 mg 100 g^{-1}), was higher than that in ZU3 and in PB. Despite some differences, the habitat conditions at both study sites were favourable for the growth of indigo bush and its accompanying native species.

The PI_{ABS} (Fig. 1*A*) was significantly lower in indigo bush than that in common oak and black alder at all three sites at PB in May. In July, a significant increase of PI_{ABS} in almost all investigated species was observed, except black alder at PB2 site. At ZU (Fig. 1*B*), indigo bush showed significantly lower PI_{ABS} compared to white poplar and common dogwood in May. In July, a significant increase of PI_{ABS} was observed only in indigo bush.

At both locations (PB and ZU), considerable increase of ΔDF_{ABS} in indigo bush compared to accompanying species was observed. The increase of PI_{ABS} in indigo bush at all sites (Fig. 2) in July, came from the increase of two partial DFs: $\log \psi_{E0}/(1-\psi_{E0})$ and $\log \gamma_{RC}/(1-\gamma_{RC})$. Negative values of ΔDF_{ABS} observed in black alder at PB2 and white poplar at ZU2 came from the decrease of $\log \gamma_{RC}/(1-\gamma_{RC})$ and $\log \varphi_{P0}/(1-\varphi_{P0})$, while in common dogwood $\log \psi_{E0}/(1-\psi_{E0})$ decreased at ZU3. The increase of PI_{ABS} in common oak at all three sites (Fig. 2*A*) at PB as well as the increase of PI_{ABS} in black alder at PB2 (Fig. 2*A*) were mainly due to the increase of $\log \psi_{E0}/(1-\psi_{E0})$.

Parameters SFI_{ABS}, φ_{P0}, φ_{E0}, φ_{R0}, ψ_{E0}, and δ_{R0} as well as specific photosynthetic fluxes per Q_A^- reducing PSII RC (Fig. 3) were derived by the JIP-test, normalised to their respective controls (measurements in May for each species), and represented as spider plots for each investigated site. The increase of SFI_{ABS} parameter in July was observed in indigo bush at all sites in both PB and ZU. Unlike the ZU (Fig. 3*D–F*), where the SFI_{ABS} did not changed in accompanying species in July, SFI_{ABS} values increased in black alder at PB3, and common oak (Fig. 3*A–C*) at all sites compared to May measurements.

In July, the values of φ_{P0}, φ_{E0}, and φ_{R0} increased significantly in indigo bush at all six sites compared to measurements in May (Fig. 3). At ZU, a significant increase was observed also in accompanying species but in a lower manner than that in indigo bush. In particular, at site ZU1, φ_{E0} and φ_{R0} increased in white poplar and at ZU3, φ_{P0} increased in common dogwood. At PB1, φ_{P0}, φ_{E0},

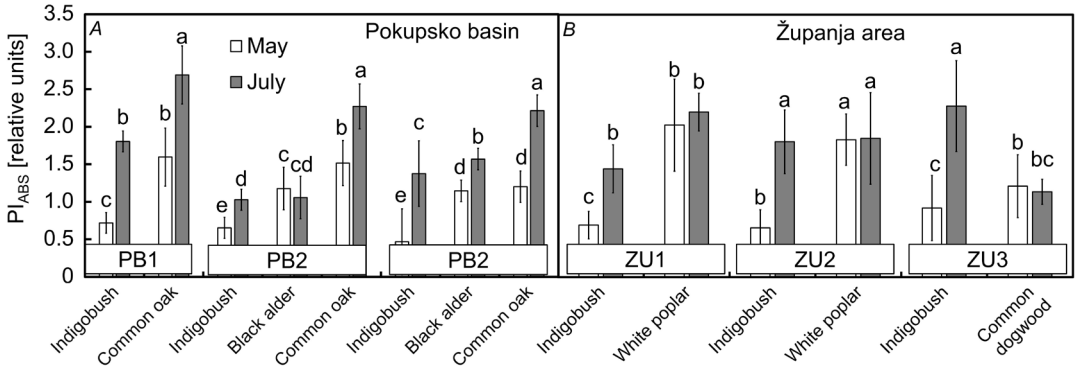

Fig. 1. Performance index (PI_{ABS}) of indigo bush and accompanying species at Pokupsko basin (*A*) and Županja area (*B*) measured in May and July. Represented values are the mean ± SD of 25 replicates; *different letters* represent significant difference at p<0.05 (*ANOVA* LSD).

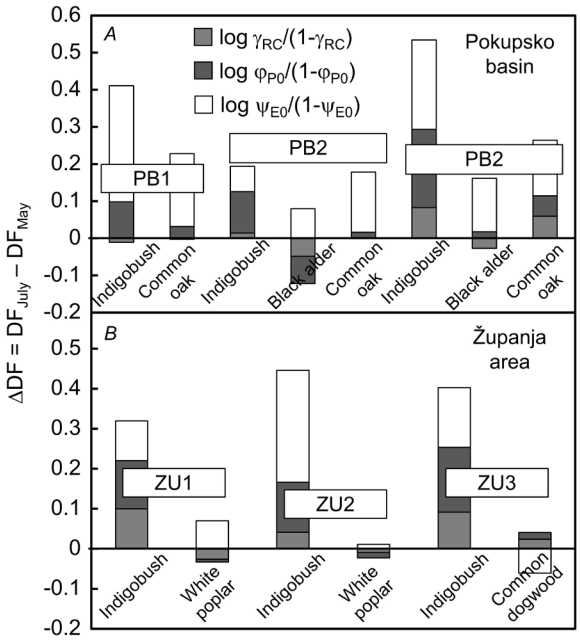

Fig. 2. Relative changes in the difference of driving forces (ΔDF) of indigo bush and accompanying species at Pokupsko basin (*A*) and Županja area (*B*). Each DF_{ABS} is calculated by summing up their partial driving forces: $\log\gamma_{RC}/(1-\gamma_{RC})$, $\log\varphi_{P0}/(1-\varphi_{P0})$, and $\log\psi_{E0}/(1-\psi_{E0})$. Represented values are the mean of 25 replicates. The difference was calculated as $\Delta DF_{ABS} = DF_{July} - DF_{May}$.

and φ_{R0} increased in common oak. At PB2, φ_{E0} and φ_{R0} increased, and φ_{P0} decreased in black alder, while φ_{E0} and φ_{R0} increased in common oak without a change in φ_{P0}. At PB3, φ_{E0} and φ_{R0} increased in black alder, and all three parameters increased in common oak.

The value of ψ_{E0} increased in indigo bush at all six sites in July (Fig. 3). Accompanying species also showed an increase in this parameter in July at ZU1, PB1, PB2, and PB3 sites, while at ZU3, it decreased compared to measurements in May. The values of δ_{R0} (Fig. 3) decreased in indigo bush at ZU2 and ZU3 sites in July, while accompanying species showed various trends. Values increased at ZU2 and decreased at ZU1 and ZU3 compared to May measurements. At PB, all accompanying species showed a significant decrease of this parameter in July compared to May measurements, except for common oak at PB1 and PB2 that showed no changes.

Indigo bush showed a decrease of certain specific energy fluxes per O_A^- reducing PSII RC (Fig. 3), namely ABS/RC, TR_0/RC, and DI_0/RC at all three sites at ZU in July compared to May measurements. Parameter ET_0/RC increased in indigo bush at ZU2 and ZU3, while RE_0/RC decreased in ZU1 and ZU3 in July. Accompanying species at ZU showed various responses in July compared to May measurements: white poplar showed an increase in ABS/RC, DI_0/RC, TR_0/RC, and ET_0/RC at ZU1 and a decrease only in the RE_0/RC parameter at ZU2. Contrary to that, common dogwood at ZU3 revealed a decrease of all specific energy fluxes. At PB, specific energy fluxes considerably varied in all species compared to the measurements in May. At PB1, the decrease of DI_0/RC with a parallel increase in TR_0/RC, ET_0/RC, and RE_0/RC in indigo bush, as well as increase in ET_0/RC and RE_0/RC in common oak, were observed. At PB2, the decrease of ABS/RC, DI_0/RC, and RE_0/RC and increase in TR_0/RC, and ET_0/RC in indigo bush can be seen. In common oak, parameters ET_0/RC and RE_0/RC increased, while in black alder, ABS/RC, DI_0/RC, TR_0/RC, and ET_0/RC increased. At PB3, ABS/RC, DI_0/RC, TR_0/RC, and RE_0/RC decreased in indigo bush and common oak. Parameter ET_0/RC increased in indigo bush, while in black alder parameters ABS/RC, TR_0/RC, and ET_0/RC increased.

Differences in average variable fast fluorescence transients (Fig. 4) were created by subtracting the normalised fluorescence values between O- and P-steps measured in May (control plants) from those measured in July ($\Delta W_t = W_{t(July)} - W_{t(May)}$) to compare major changes occurring in the O–J and O–I phases in indigo bush and accompanying native species. At PB (Fig. 4*A*), negative peaks at J-step can be seen in all species except black alder at PB2. Positive amplitudes at I-step were observed in all species except black alder at PB3. At ZU (Fig. 4*D*), indigo bush plants showed negative peaks at J-step and positive peaks at I-step. All three accompanying species revealed positive peaks around I-step.

The O–J and O–K normalised curves revealed K- (Fig. 4*B*,*E*) and L-bands (Fig. 4*C*,*F*), respectively. At PB, negative K-band (Fig. 4*B*) was observed in indigo bush at PB2 and in indigo bush and common oak at PB3. Indigo bush at PB1 showed negative K-band with the least expressed amplitudes followed by the positive inflexion afterwards. Black alder showed the positive K-band at both PB2 and PB3. At ZU (Fig. 4*E*), indigo bush plants revealed negative K-bands at all three sites. The negative K-band was also observed at common dogwood at ZU3, while white poplar at ZU1 and ZU2 showed the positive K-bands. The most pronounced negative L-bands at PB (Fig. 4*C*) were seen in indigo bush at all three sites as well as in common oak at PB3. The most pronounced positive amplitude was observed in black alder at PB2. At ZU (Fig. 4*F*), indigo bush revealed the most pronounced negative L-bands while accompanying species revealed only minor inflexions.

Discussion

Comparison between the native and non-native species represents the most important approach to determine the mechanisms associated with the alien success (Ordonez *et al.* 2010). Some previous studies showed that plant invasiveness may be achieved by their effective photosynthesis (Baležentienė 2019). For example, the invasive *Rubus discolour* and *R. laciniatus* showed significantly higher photosynthetic capacity and maintained net photosynthesis over a longer period of the year than that of the noninvasive *R. ursinus* and *R. leucodermis* (McDowell 2002). Also, the superior invasiveness of *Impatiens glandulifera* in comparison with noninvasive *I. parviflora* could be related to its better photosynthetic characteristics

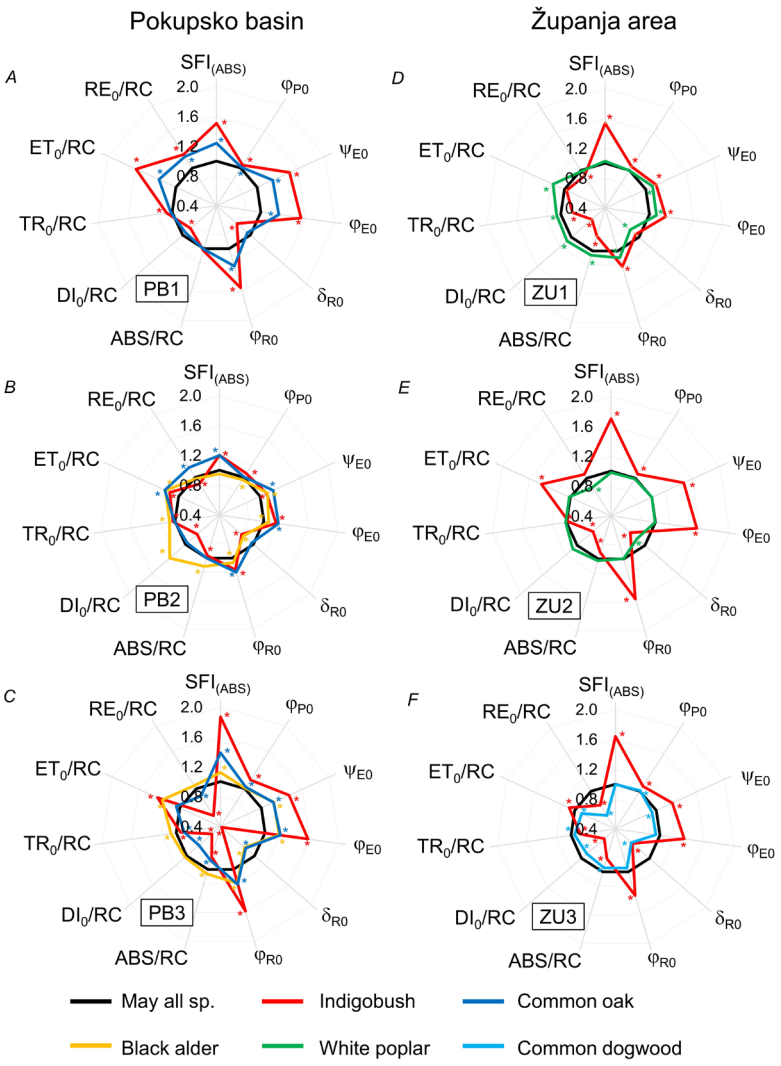

Fig. 3. Spider plots of normalised values of selected chlorophyll *a* fluorescence parameters characterising PSII functioning in indigo bush and accompanying species at Pokupsko basin (*A–C*) and Županja area (*D–F*). All values are shown as difference for each species, compared to the measurements in May (May = 1; *black line*). Each curve represents average kinetics of 25 replicates per species. *Asterisks* (*) represent significant difference at $p<0.05$ (*ANOVA* LSD) for each species (different colour) in comparison to measurements in May. $SFI_{(ABS)}$ – structure–function index on absorption basis; φ_{P0} – maximum quantum yield of primary photochemistry; ψ_{E0} – probability of electron transport further than Q_A^-; φ_{E0} – quantum yield of electron transfer further than Q_A^-; δ_{R0} – probability for an electron from the intersystem carriers reduces terminal electron acceptors at the PSI acceptor side; φ_{R0} – quantum yield for the reduction of terminal electron acceptors at the PSI acceptor side; ABS/RC – absorption flux per active RC; DI_0/RC – dissipation flux per active RC; TR_0/RC – trapping flux per active RC; ET_0/RC – electron transport flux per active RC; RE_0/RC – electron flux reducing end terminal electron acceptors at the PSI acceptor side, per RC.

such as light harvesting and carbon fixation (Ugoletti *et al.* 2011).

The results of our study showed the intra- and inter-specific differences in photosynthetic performance of the investigated plants – the invasive indigo bush and the native accompanying shrubs and trees originating from different families but sharing the same ecological niche. Generally, the variability in photosynthetic performance could be connected to plants genetic features but also may depend on the different environmental conditions (*e.g.*, soil characteristics, precipitation) occurring in their habitats. The soil properties as well as the content of nitrogen and phosphorus in the soil may control photosynthesis through the accumulation of minerals in leaves (Maire *et al.* 2015, Shi *et al.* 2017). The low nutrient supply may reduce photosynthesis in some plant species (*e.g.*, *Quercus petraea*) (Kazda *et al.* 2004). Precipitation also has an important role. The well-watered conditions positively affect plant photosynthetic rates and consequently influence their growth (Ramírez-Valiente *et al.* 2017). It has been found that the net photosynthetic rate of indigo bush seedlings declined in the conditions of inadequate water supply (Zhang *et al.* 2013). However, in natural conditions, it is difficult to distinguish the influence and importance of individual factors on plant development.

Fully developed indigo bush plants at both study sites, forest habitats in PB as well as in lowland areas of ZU, had more efficient photosynthetic performance (a higher increase of PI_{ABS} and DF_{ABS}) in July compared to accompanying species. PI_{ABS} increased due to the increase in all of the three partial driving forces but especially in indigo bush ability to convert excitation energy to electron transport chain beyond primary acceptor [$\log \psi_{E0}/(1 - \psi_{E0})$]. This indicates that indigo bush may increase its ability of energy conservation in summer (Yusuf *et al.* 2010, Dąbrowski *et al.* 2019). Additionally, this invasive plant had the negative L-band which could be associated with better energetic connectivity between the PSII and its RCs (Chen and Cheng 2009) while negative inflexion of K-band indicated substantial speeding of electron flow between OEC and acceptor side of the RC (Oukarroum *et al.* 2007, Yusuf *et al.* 2010). Indigo bush utilisation of absorbed light energy was highly efficient. It was evident in an increase of specific energy fluxes per

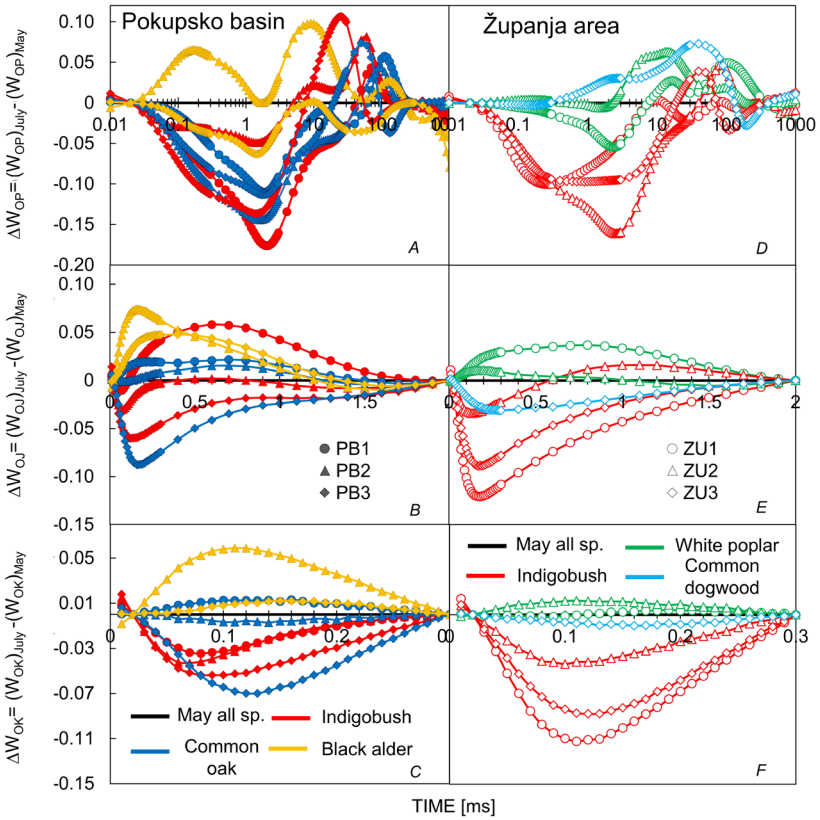

Fig. 4. Changes in the shape of the chlorophyll *a* fluorescence transient curves for indigo bush and accompanying species at Pokupsko basin (*A–C*) and Županja area (*D–F*). Each curve represents average kinetics of 25 replicates. Average fluorescence data were normalised to compare specific events in the O–P (*A*,*D*), O–J (K-band) (*B*,*E*), and O–K (L-band) (*C*,*F*) phases in the recorded OJIP transients. The difference (ΔW_{OP}, ΔW_{OJ}, and ΔW_{OK}) in the relative variable fluorescence was calculated as $\Delta W_t = W_{t(July)} - W_{t(May)}$ for each species.

Q_A^- reducing PSII RC, especially electron transport (ET_0/RC), and trapping (TR_0/RC), while simultaneously, energy dissipation decreased (DI_0/RC). Although the indigo bush plants enhanced photosynthetic efficacy at both PB and ZU in July, some differences were observed. At all three sites in PB – maximum quantum efficiency of the primary photochemistry (φ_{P0}), the quantum yield for electron transport (φ_{E0}), and the reduction of terminal electron acceptor at PSI acceptor side (φ_{R0}) as well as the efficiency of electron transport further than Q_A^- (ψ_{E0}) substantially increased. At the same time, at all three sites in ZU, indigo bush decreased absorption, trapping and dissipation per RC but increased quantum yields and efficiencies. Such results suggested improved electron flow from Q_A^- all the way to the acceptors at PSI (Krüger *et al.* 2014). It was reported recently that invasive *Acacia* species exhibited higher φ_{P0} values than that of native species (Le *et al.* 2019) suggesting better light harvesting and greater plasticity of PSII. In this way, invasive *Acacia* species were able to adjust photosynthetic apparatus better to broad temperature range than native forest tree species. Such results suggested the greater plasticity of indigo bush in our investigation. Indigo bush had very high values of the structure–function index (SFI_{ABS}), a combination of functional and structural criteria that describes PSII (Goltsev *et al.* 2016, Mathur *et al.* 2016, Stirbet *et al.* 2018). High values indicated the strong influence of the internal factors that promote efficient reactions within PSII. The increase of SFI_{ABS} in July confirmed efficient use of absorbed light energy within active PSII RCs. It was argued that utilizing more energy for photochemistry could help invasive plants to avoid possible photodamage or to protect photosynthetic apparatus more efficiently than native species (Feng *et al.* 2007). Such results indicated that investigated invasive species could protect their photosynthetic apparatus mainly through use of absorbed light energy rather than by thermal dissipation.

The common oak had higher photosynthetic performance in May but in July, a higher increase of PI_{ABS} values was observed in indigo bush. Earlier measurements of maximum efficiency of PSII (F_v/F_m) indicated a slow development of maximum photosynthetic capacity in common oak plants (Morecroft *et al.* 2003). This could be related to a variety of processes in this plant species, including the formation of ring-porous trees what may reduce the availability of resources necessary for leaf development. Additionally, it corresponds to the synthesis of a high amount of phenolic compounds that may divert some resources away from complete development of photosynthetic performance. Although lesser than in indigo bush, the photosynthetic performance of common oak plants continuously increased especially in terms of quantum yields (φ_{P0}, φ_{E0}, and φ_{R0}) and efficiency (ψ_{E0}) as well as partial DF log $\psi_{E0}/(1 - \psi_{E0})$ which was the main reason for the increase of DF_{ABS} in investigated plants. Positive inflexions of L- and K-bands in common oak at PB1 and PB2 were not considered significant, but noticeably negative L- and K-bands at PB3 suggested that common oak plants could maintain thriving photosynthetic efficiency from May to July. Our results showed that both

species maintained efficient photosynthesis due to efficient electron transport. This implied that somewhat different strategies were needed to maintain efficient photosynthesis in indigo bush and common oak. Recent investigation on native *Robinia pseudoacacia* and invasive *A. fruticosa* showed that both species had similar F_v/F_m values. This suggested that both species were able to stabilize photosynthetic performance under stressful conditions (Guo *et al.* 2018). However, *R. pseudoacacia* showed constant of energy dissipation with the increase of stress level while in *A. fruticosa* dissipation increased. Such results implied that both investigated species had certain resistance to stressful conditions but developed different strategies to maintain efficient photosynthesis.

The photosynthetic performance of black alder grown at different habitats showed significant variability and was not as successful in maintaining the photosynthetic performance as indigo bush and common oak. At PB2, black alder PI_{ABS} remained at the same level in July as in May. The maximum quantum yield for primary photochemistry (φ_{P0}) decreased, what was followed by the increase of absorption, trapping, and dissipation per active RC, indicating that particular part of RCs undergo structural transformation and became non-Q_A-reducing or 'silent' ones (Gonçalves *et al.* 2007, Yusuf *et al.* 2010). Additionally, positive L- and K-bands observed could be related to low system connectivity and inactivation of the OEC (Yusuf *et al.* 2010, Dąbrowski *et al.* 2016). This indicates that less energy has been exchanged between PSII units as well as the poor ability of black alder for using absorbed light energy for reducing Q_A. It was suggested recently that invasive species *Rhus thypina* showed increased light acquisition and higher photosynthesis in comparison to native *Vitex negundo* which contributed to the higher plant growth of invasive species (Tan *et al.* 2018).

The white poplar had the higher maximum quantum efficiency for primary photochemistry and overall performance index in May than that of indigo bush. However, while performance significantly increased in indigo bush in July, white poplar maintained its performance throughout the investigation. Nevertheless, small deviations in other parameters were observed in white poplar. Namely, electron transport per active RCs, φ_{E0} and φ_{R0} as well as the ψ_{E0}, increased in July at ZU1 but to a lesser extent compared to the response of indigo bush. Similarly, two invasive *Rubus* species showed higher electron transport rate compared to native ones. Invasive species maintained photosynthetic capacity throughout the year what enabled them to allocate greater amount of carbon. Consequently, a higher capacity for photosynthesis of invasive *Rubus* lead to their higher growth rates compared to native species (McDowell 2002). Such results correspond to ours since both species at ZU1 showed the increase of electron transport but with the greater increase in indigo bush. Additionally, at ZU2, all named parameters measured in white poplar remained at the same level. White poplar decreased the RC density and primary photochemistry in July at both Županja sites, which can be seen as negative partial DF for $\log \gamma_{RC}/(1 - \gamma_{RC})$ and $\log \varphi_{P0}/(1 - \varphi_{P0})$ when compared to the response of indigo bush in July.

Common dogwood showed an increase in RC density and primary photochemistry parameters in July but a significant decrease in $\log \psi_{E0}/(1 - \psi_{E0})$ values, suggesting that contribution of efficient redox reaction between PSII and PSI was considerably reduced (Tsimilli-Michael and Strasser 2008, Krüger *et al.* 2014). Additionally, common dogwood revealed a decrease of all specific energy fluxes per reducing Q_A^- RCs as well as efficiencies for electron transport between Q_A^- and Q_B and further (ψ_{E0} and δ_{R0}), while φ_{P0} increased what could be the result of lower quantity of active PSII RCs (Chen and Cheng 2009). Nonsignificant changes of L- and K-bands indicate a rather stabile reaction, as it was also found in white poplar. On the other side, both bands in indigo bush revealed negative inflexions at all three Županja sites suggesting significant improvement of the system connectivity, faster electron transport (Pollastrini *et al.* 2017), and the ability to utilize efficiently absorbed energy (Oukarroum *et al.* 2007, Yusuf *et al.* 2010) compared to May measurements, as well as compared to white poplar and common dogwood. Recent investigation on *R. pseudoacacia* and *A. fruticosa*, native and invasive species, showed that *A. fruticosa* had more efficient electron transport compared to *R. pseudoacacia* what enabled *A. fruticosa* to gain higher biomass (Guo *et al.* 2018).

Conclusions: By monitoring changes and differences in photosynthetic parameters that characterize the functioning of plants at the canopy level, we gained insight into adjustments of photosynthetic apparatus in indigo bush and dominant native species from the beginning of the vegetation period in May until the flowering period in July. Our results suggested that indigo bush was able to use absorbed light energy for electron transport more efficiently than accompanying native species. Negative L- and K-bands implied a good connectivity within the PSII units as well as a faster electron transport. An increase of parameters φ_{P0}, φ_{E0}, φ_{R0}, ψ_{E0}, and ET_0/RC followed by lower DI_0/RC in indigo bush in July at all six sites additionally confirmed enhanced electron transport from PSII forward to PSI. Moreover, the increase of PI_{ABS} and SFI_{ABS} in indigo bush in July suggested the efficient utilisation of absorbed light energy. Such results imply that indigo bush could protect its photosynthetic apparatus mainly through efficient utilising absorbed light energy rather than through thermal dissipation. Even though chosen accompanying species followed pace with indigo bush plants in most discussed parameters to some extent, indigo bush revealed a remarkable plasticity of photosynthetic reactions. More effective capture and utilisation of light resources may be important factors that contribute to the successful adaptation of this invasive species. To our knowledge, this is the first comparative study of photosynthetic performance of indigo bush and its accompanying native species in the field. Thus, further investigations are necessary to get an elaborate insight into the functioning and acclimatization of their photosynthetic apparatus to natural environmental conditions that lead to increase of biomass and faster growth. These results could contribute

to a better understanding of photosynthetic mechanisms that play a role in the success of this invasive species and additionally, for the development of appropriate control strategies.

References

Bajwa A.A., Chauhan B.S., Farooq M. *et al.*: What do we really know about alien plant invasion? A review of the invasion mechanism of one of the world's worst weeds. – Planta **244**: 39-57, 2016.

Baležentienė L.: Germination response to phytotoxicity of *Impatiens parviflora*. – Biologija **65**: 34-40, 2019.

Begović L., Mlinarić S., Antunović Dunić J. *et al.*: Response of *Lemna minor* L. to short-term cobalt exposure: The effect on photosynthetic electron transport chain and induction of oxidative damage. – Aquat. Toxicol. **175**: 117-126, 2016.

Brigić A., Vujčić-Karlo S., Matoničkin Kepčija R. *et al.*: Taxon specific response of carabids (Coleoptera, Carabidae) and other soil invertebrate taxa on invasive plant *Amorpha fruticosa* in wetlands. – Biol. Invasions **16**: 1497-1514, 2014.

Bussotti F., Pollastrini M.: Observing climate change impacts on European forests: What works and what does not in ongoing long-term monitoring networks. – Front. Plant. Sci. **8**: 629, 2017.

Chen L.-S., Cheng L.: Photosystem 2 is more tolerant to high temperature in apple (*Malus domestica* Borkh.) leaves than in fruit peel. – Photosynthetica **47**: 112-120, 2009.

Csiszár Á., Korda M., Schmidt D. *et al.*: Allelopathic potential of some invasive plant species occurring in Hungary. – Allelopathy J. **31**: 309-318, 2013.

Dąbrowski P., Baczewska-Dąbrowska A.H., Kalaji H.M. *et al.*: Exploration of chlorophyll *a* fluorescence and plant gas exchange parameters as indicators of drought tolerance in perennial ryegrass. – Sensors-Basel **19**: 2736, 2019.

Dąbrowski P., Baczewska A.H., Pawluśkiewicz B. *et al.*: Prompt chlorophyll *a* fluorescence as a rapid tool for diagnostic changes in PSII structure inhibited by salt stress in Perennial ryegrass. – J. Photoch. Photobio. B **157**: 22-31, 2016.

DeHaan L.R., Ehlke N.J., Sheaffer C.C. *et al.*: Evaluation of diversity among North American accessions of false indigo (*Amorpha fruticosa* L.) for forage and biomass. – Genet. Resour. Crop Ev. **53**: 1463-1476, 2006.

Dogra K.S., Sood S.K., Dobhal P.K. *et al.*: Alien plant invasion and their impact on indigenous species diversity at global scale: A review. – J. Ecol. Nat. Environ. **2**: 175-186, 2010.

Dudeque Zenni R., Lacerda da Cunha W., Sena G.: Rapid increase in growth and productivity can aid invasions by a non-native tree. – AoB Plants **8**: plw048, 2016.

Egnér H., Riehm H., Domingo W.: [Investigations about the chemical soil analysis as a basis for the distribution nutrient condition of the soil. II. Chemical extraction methods for phosphorus and potassium production.] Untersuchungen über die chemische Bodenanalyse als Grundlage für die Beurteilung des Nährstoffzustandes der Böden. II. Chemische Extraktionsmethoden zur Phosphor-und Kaliumbestimmung. – Kungliga Lantbrukshögskolans Annaler **26**: 199-215, 1960. [In German]

Feng Y.-L., Wang J.-F., Sang W.-G.: Irradiance acclimation, capture ability, and efficiency in invasive and non-invasive alien plant species. – Photosynthetica **45**: 245-253, 2007.

Genovesi P., Scalera R., Brunel S. *et al.*: Towards an early warning and information system for invasive alien species (IAS) threatening biodiversity in Europe. Pp. 47. European Environment Agency, Copenhagen 2010.

Goltsev V.N., Kalaji H.M., Paunov M. *et al.*: Variable chlorophyll fluorescence and its use for assessing physiological condition of plant photosynthetic apparatus. – Russ. J. Plant Physl+ **63**: 869-893, 2016.

Gonçalves J.F.C., Santos Jr. U.M., Nina Jr. A.R., Chevreuil L.R.: Energetic flux and performance index in copaiba (*Copaifera multijuga* Hayne) and mahogany (*Swietenia macrophylla* King) seedlings grown under two irradiance environments. – Braz. J. Plant Physiol. **19**: 171-184, 2007.

Govindjee: Chlorophyll *a* fluorescence: A bit of basic and history. – In: Papageorgiou G.C., Govindjee (ed.): Chlorophyll *a* Fluorescence: A Signature of Photosynthesis. Pp. 1-42. Springer, Dordrecht 2004.

Gudžinskas Z., Žalneravičius E.: Notes on alien plant species *Amorpha fruticosa* new to Lithuania. – Bot. Lith. **21**: 160-165, 2015.

Guo X., Ren X.-H., Eller F. *et al.*: Higher phenotypic plasticity does not confer higher salt resistance to *Robinia pseudoacacia* than *Amorpha fruticosa*. – Acta Physiol. Plant. **40**: 79, 2018.

Hejda M., Pyšek P., Jarošík V.: Impact of invasive plants on the species richness, diversity and composition of invaded communities. – J. Ecol. **97**: 393-403, 2009.

Horvat G., Franjić J.: [Invasive plants of Kalnik forests.] Invazivne biljke Kalničkih šuma. – Sumar. List **140**: 53-64, 2016. [In Croatian] doi: 10.31298/sl.140.1-2.6.

Jakovljević T., Halambek J., Radošević K. *et al.*: The potential use of Indigobush (*Amorpha fruticosa* L.) as natural resource of biologically active compounds. – SEEFOR **6**: 171-178, 2015.

Kalaji H., Rastogi A., Živčák M. *et al.*: Prompt chlorophyll fluorescence as a tool for crop phenotyping: an example of barley landraces exposed to various abiotic stress factors. – Photosynthetica **56**: 953-961, 2018.

Kazda M., Salzer J., Schmid I., von Wrangell P.: Importance of mineral nutrition for photosynthesis and growth of *Quercus petraea*, *Fagus sylvatica* and *Acer pseudoplatanus* planted under Norway spruce canopy. – Plant Soil **264**: 25-34, 2004.

Keane R.M., Crawley M.J.: Exotic plant invasions and the enemy release hypothesis. – Trends Ecol. Evol. **17**: 164-170, 2002.

Keller R.P., Geist J., Jeschke J.M., Kühn I.: Invasive species in Europe: ecology, status, and policy. – Environ. Sci. Eur. **23**: 23, 2011.

Krüger G.H.J., De Villiers M.F., Strauss A.J. *et al.*: Inhibition of photosystem II activities in soybean (*Glycine max*) genotypes differing in chilling sensitivity. – S. Afr. J. Bot. **95**: 85-96, 2014.

Küpper H., Benedikty Z., Morina F. *et al.*: Analysis of OJIP chlorophyll fluorescence kinetics and Q_A reoxidation kinetics by direct fast imaging. – Plant Physiol. **179**: 369-381, 2019.

Le Q.-V., Tennakoon K.U., Metali F., Sukri R.S.: Photosynthesis in co-occurring invasive *Acacia* spp. and native Bornean heath forest trees at the post-establishment invasion stage. – J. Sustain. Forest. **38**: 230-243, 2019.

Levine J.M., Vilà M., D'Antonio C.M. *et al.*: Mechanisms underlying the impacts of exotic plant invasions. – P. Roy. Soc. Lond. B Bio. **270**: 775-781, 2003.

Luo X., Xu X., Zheng Y. *et al.*: The role of phenotypic plasticity and rapid adaptation in determining invasion success of *Plantago virginica*. – Biol. Invasions **21**: 2679-2692, 2019.

Maire V., Wright I.J., Prentice I.C. *et al.*: Global effects of soil and climate on leaf photosynthetic traits and rates. – Global Ecol. Biogeogr. **24**: 706-717, 2015.

Mathur S., Kalaji H.M., Jajoo A.: Investigation of deleterious effects of chromium phytotoxicity and photosynthesis in wheat plant. – Photosynthetica **54**: 185-192, 2016.

Mayer K., Haeuser E., Dawson W. *et al.*: Naturalization of ornamental plant species in public green spaces and private

gardens. – Biol. Invasions **19**: 3613-3627, 2017.
McDowell S.C.L.: Photosynthetic characteristics of invasive and noninvasive species of *Rubus* (Rosaceae). – Am. J. Bot. **89**: 1431-1438, 2002.
Mitrović M., Jarić S., Kostić O. *et al.*: Photosynthetic efficiency of four woody species growing on fly ash deposits of a Serbian 'Nikola Tesla-A' thermoelectric plant. – Pol. J. Environ. Stud. **21**: 1339-1347, 2012.
Mlinarić S., Antunović Dunić J., Skendrović Babojelić M. *et al.*: Differential accumulation of photosynthetic proteins regulates diurnal photochemical adjustments of PSII in common fig (*Ficus carica* L.) leaves. – J. Plant Physiol. **209**: 1-10, 2017.
Mlinarić S., Antunović Dunić J., Štolfa I. *et al.*: High irradiation and increased temperature induce different strategies for competent photosynthesis in young and mature fig leaves. – S. Afr. J. Bot. **103**: 25-31, 2016.
Morecroft M.D., Stokes V.J., Morison J.I.L.: Seasonal changes in the photosynthetic capacity of canopy oak (*Quercus robur*) leaves: the impact of slow development on annual carbon uptake. – Int. J. Biometeorol. **47**: 221-226, 2003.
Ordonez A., Wright I.J., Olff H.: Functional differences between native and alien species: a global scale comparison. – Funct. Ecol. **24**: 1353-1361, 2010.
Oukarroum A., El Madidi S., Schansker G., Strasser R.J.: Probing the responses of barley cultivars (*Hordeum vulgare* L.) by chlorophyll *a* fluorescence OLKJIP under drought stress and re-watering. – Environ. Exp. Bot. **60**: 438-446, 2007.
Papageorgiou G.C.: Fluorescence of photosynthestic pigments *in vitro* and *in vivo*. – In: Papageorgiou G.C., Govindjee (ed.): Chloprphyll *a* Fluorescence: A Signature of Photosynthesis. Pp. 43-63. Springer, Dordrecht 2004.
Petrović J., Ćurčić S., Stavretović N.: [Invasive plant species and ecological factors influencing the spreading in the area of the Obrenovački Zabran Nature Monument (Central Serbia).] – Sumar. List **140**: 45-51, 2016. [In Croatian] doi: 10.31298/sl.140.1-2.5.
Pokos N., Turk I.: [Geographic characteristics of Vukovar-Syrmia County.] – In: (ed.): Vukovarsko-srijemska županija – Prostor, ljudi, identitet. Institut društvenih znanosti Ivo Pilar, Vukovarsko-srijemska županija 2012. [In Croatian]
Pollastrini M., Nogales A.G., Benavides R. *et al.*: Tree diversity affects chlorophyll *a* fluorescence and other leaf traits of tree species in a boreal forest. – Tree Physiol. **37**: 199-208, 2017.
Ramírez-Valiente J.A., Center A., Sparks J.P. *et al.*: Population-level differentiation in growth rates and leaf traits in seedlings of the neotropical live oak *Quercus oleoides* grown under natural and manipulated precipitation regimes. – Front. Plant Sci. **8**: 585, 2017.
Sărăţeanu V.: Assessing the influence of *Amorpha fruticosa* L. invasive srub species on some grassland vegetation types from western Romania. – Res. J. Agric. Sci. **42**: 563-540, 2010.
Schansker G., Tóth S.Z., Holzwarth A.R., Garab G.: Chlorophyll *a* fluorescence: beyond the limits of the Q_A model. – Photosynth. Res. **120**: 43-58, 2014.
Shi G., Ma C.: [Biological characteristics of alien plants successful invasion.] – Chin. J. Appl. Ecol. **17**: 727-732, 2006. [In Chinese]
Shi Q., Yin Y., Wang Z. *et al.*: Influence of soil properties on the performance of the *Taxodium* hybrid 'Zhongshanshan 407' in a short-term pot experiment. – Soil Sci. Plant Nutr. **63**: 145-152, 2017.
Song L., Chow W.S., Sun L. *et al.*: Acclimation of photosystem II to high temperature in two *Wedelia* species from different geographical origins: implications for biological invasions upon global warming. – J. Exp. Bot. **61**: 4087-4096, 2010.
Stirbet A., Lazár D., Kromdijk J., Govindjee: Chlorophyll *a* fluorescence induction: Can just a one-second measurement be used to quantify abiotic stress responses? – Photosynthetica **56**: 86-104, 2018.
Strasser R.J., Srivastava A., Tsimilli-Michael M.: The fluorescence transient as a tool to characterize and screen photosynthetic samples. – In: Yunus M., Pathre U., Mohanty P. (ed.): Probing Photosynthesis: Mechanisms, Regulation and Adaptation. Pp. 445-483. Taylor & Francis, London 2000.
Strasser R.J., Tsimilli-Michael M., Srivastava A.: Analysis of the chlorophyll *a* fluorescence transient. – In: Papageorgiou G.C., Govinjee (ed.): Chlorophyll *a* Fluorescence: A Signature of Photosynthesis. Pp. 321-362. Springer, Dordrecht 2004.
Tan X., Guo X., Guo W. *et al.*: Invasive *Rhus typhina* invests more in height growth and traits associated with light acquisition than do native and non-invasive alien shrub species. – Trees **32**: 1103-1112, 2018.
Tsimilli-Michael M., Strasser R.J.: *In vivo* assessment of stress impact on plants' vitality: applications in detecting and evaluating the beneficial role of mycorrhization on host plants. – In: Varma A. (ed.): Mycorrhiza. State of the Art, Genetics and Molecular Biology, Eco-Function, Biotechnology, Eco-Physiology, Structure and Systematics. 3rd Edition. Pp. 679-703. Springer, Berlin-Heidelberg 2008.
Ugoletti P., Stout J.C., Jones M.B.: Ecophysiological traits of invasive and non-invasive introduced *Impatiens* species. – In: Biology and Environment: Proceedings of the Royal Irish Academy. Vol. 111B. Pp. 143-156. Royal Irish Academy 2011.
Vilà M., Basnou C., Pyšek P. *et al.*: How well do we understand the impacts of alien species on ecosystem services? A pan-European, cross-taxa assessment. – Front. Ecol. Environ. **8**: 135-144, 2010.
Vincetić M., Žuna Pfeiffer T., Krstin L. *et al.*: [Spreading of invasive species *Amorpha fruticosa* L. in the area of Županja.] – In: 10th International Scientific/Professional Conference, Agriculture in Nature and Environment Protection, 5–7 June 2017, Vukovar, Croatia. Pp. 167-172, 2017. [In Croatian]
Yusuf M.A., Kumar D., Rajwanshi R. *et al.*: Overexpression of γ-tocopherol methyl transferase gene in transgenic *Brassica juncea* plants alleviates abiotic stress: physiological and chlorophyll *a* fluorescence measurements. – BBA-Bioenergetics **1797**: 1428-1438, 2010.
Zhang X.-R., Tan X.-F., Wang R.-Q. *et al.*: Effects of soil moisture and light intensity on ecophysiological characteristics of *Amorpha fruticosa* seedlings. – J. Forestry Res. **24**: 293-300, 2013.
Zhao L.-S., Li K., Wang Q.-M. *et al.*: Nitrogen starvation impacts the photosynthetic performance of *Porphyridium cruentum* as revealed by chlorophyll *a* fluorescence. – Sci. Rep.-UK **7**: 8542, 2017.
Zhou R., Yu X., Kjær K.H. *et al.*: Screening and validation of tomato genotypes under heat stress using F_v/F_m to reveal the physiological mechanism of heat tolerance. – Environ. Exp. Bot. **118**: 1-11, 2015.
Žuna Pfeiffer T., Štolfa Čamagajevac I., Špoljarić Maronić D. *et al.*: Regulation of photosynthesis in algae under metal stress. – In: Singh R., Singh V., Singh S. *et al*. (ed.): Environment and Photosynthesis: A Future Prospect. Pp. 261-286. Studium Press, New Delhi 2018.

Appendix. Calculations and descriptions of parameters used by JIP-test.

Recorded data, technical and calculated parameters	Description
F_t	Fluorescence at any time *t* after the onset of actinic illumination
$F_0 \cong F_{20\mu s}$	Minimal fluorescence
$F_m \cong F_P$	Maximal fluorescence
$F_v = F_m - F_0$	Variable fluorescence at any time *t*
$V_t = (F_t - F_0)/(F_m - F_0)$	Normalized variable fluorescence at any time *t*
$W_{OP} = (F_t - F_0)/(F_m - F_0)$	Relative variable fluorescence normalised to the amplitude at any time *t*
$W_{OJ} = (F_t - F_0)/(F_J - F_0)$	Relative variable fluorescence normalised to the amplitude of the O–J phase (K-band)
$W_{OK} = (F_t - F_0)/(F_K - F_0)$	Relative variable fluorescence normalised to the amplitude of the O–K phase (L-band)
$M_0 = (dV/dt)_0$	Approximated initial slope of relative variable fluorescence
$\varphi_{P0} = TR_0/ABS = F_v/F_m = TR_0/ABS$	Maximum quantum yield of primary photochemistry
$\varphi_{E0} = ET_0/ABS = F_v/F_m\ (1 - V_J)$	Quantum yield of electron transfer further than Q_A^-
$\varphi_{R0} = RE_0/ABS = [1 - (F_0 - F_m)]\psi_{E0}\delta_{R0}$	Quantum yield for the reduction of terminal electron acceptors at the PSI acceptor side
$\psi_{E0} = ET_0/TR_0 = 1 - V_J$	Probability of electron transport further than Q_A^-
$\delta_{R0} = RE_0/ET_0 = (1 - V_I)/(1 - V_J)$	Probability for an electron from the intersystem carriers reduces terminal electron acceptors at the PSI acceptor side
$RC/CS_0 = (ABS/CS)/(ABS/RC)$	Density of active RC per excited cross section
$ABS/RC = M_0(1/V_J)[1/(F_v/F_m)] = (TR_0/RC)/(TR_0/ABS)$	Absorption flux per active RC
$TR_0/RC = M_0(1/V_J)$	Trapping flux per active RC
$ET_0/RC = M_0(1/V_J)(1 - V_J) = (TR_0/RC)(ET_0/TR_0)$	Electron transport flux per active RC
$DI_0/RC = (ABS/RC) - (TR_0/RC)$	Dissipation flux per active RC
$RE_0/RC = M_0(1/V_J)\psi_{E0}\delta_{R0}$	Electron flux reducing end terminal electron acceptors at the PSI acceptor side, per RC
$\gamma_{RC} = Chl_{RC}/Chl_{total} = RC/(ABS + RC)$	Probability that a PSII Chl molecule functions as RC
$RC/ABS = \gamma_{RC}/(1 - \gamma_{RC}) = \varphi_{P0}(V_J/M_0)$	Density of RC on chlorophyll *a* basis
$PI_{ABS} = [\gamma_{RC}/(1 - \gamma_{RC})][\varphi_{P0}/(1 - \varphi_{P0})][\psi_{E0}/(1 - \psi_{E0})]$	Performance index on absorption basis
$DF_{ABS} = \log PI_{ABS} = [\log \gamma_{RC}/(1 - \gamma_{RC})] + [\log \varphi_{P0}/(1 - \varphi_{P0})] + + [\log \psi_{E0}/(1 - \psi_{E0})]$	Driving forces in PSII on absorption basis
$SFI_{ABS} = (RC/ABS)(TR_0/ABS)/(ET_0/TR_0)$	Structure–function index on absorption basis